

Cite this: *Digital Discovery*, 2025, 4, 403

Knowledge discovery from porous organic cage literature using a large language model†

Yaoyi Su,^{‡a} Siyuan Yang,^{‡ab} Yuanhan Liu,^a Aiting Kai,^{ab} Linjiang Chen^{*cd} and Ming Liu^{ib*ab}

Porous organic cages (POCs) are an emerging subclass of porous materials, drawing increasing attention due to their structural tunability, modularity and processibility, with the research in this area rapidly expanding. Nevertheless, it is a time-consuming and labour-intensive process to obtain sufficient information from the extensive literature on organic molecular cages. This article presents a GPT-4-based literature reading method that incorporates multi-label text classification and a follow-up information extraction, in which the potential of GPT-4 can be fully exploited to rapidly extract valid information from the literature. In the process of multi-label text classification, the prompt-engineered GPT-4 demonstrated the ability to label text with proper recall rates according to the type of information contained in the text, including authors, affiliations, synthetic procedures, surface area, and the Cambridge Crystallographic Data Centre (CCDC) number of corresponding cages. Additionally, GPT-4 demonstrated proficiency in information extraction, effectively transforming labeled text into concise tabulated data. Furthermore, we built a chatbot based on this database, allowing for quick and comprehensive searching across the entire database and responding to cage-related questions.

Received 21st October 2024
Accepted 18th December 2024

DOI: 10.1039/d4dd00337c

rsc.li/digitaldiscovery

Introduction

Porous organic cages (POCs) are an emerging subclass of porous materials, distinguished by their unique structural tunability and ease of processing. Like other porous materials, POCs have adjustable pore structures, which make them suitable for a wide range of applications, including gas adsorption and separation,^{1–4} molecular detection,^{5,6} and use as catalyst carriers.^{7–9} The pioneering work on organic cage molecules was first reported by Lehn *et al.* in 1969, where they introduced a three-dimensional cryptand for cation binding.¹⁰ It is not until 2009 that Tozawa *et al.* discovered a series of rigid imine cages exhibiting permanent porosity in the solid state.¹ Since then, significant interest has emerged in the design, synthesis, and application of POCs, which vary in their building units, shapes, and sizes.^{11,12} The synthesis of POCs is inherently complex, requiring a range of organic reactions and intricate

experimental procedures.¹³ To replicate these syntheses, researchers must refer to the detailed synthetic steps outlined in the literature. Beyond the synthesis itself, information on the specific surface area, crystal structure, and topology of POCs is essential due to its relevance to their applications. However, extracting this information from the extensive body of literature is both time-consuming and labor-intensive.

Large language models (LLMs) like Generative Pre-trained Transformer (GPT) can generate responses based on patterns and statistical principles learned during their pre-training phase.¹⁴ These models can interact dynamically, adapting to the context of a conversation to simulate human-like dialogue and communication. With hundreds of millions of parameters, GPT has shown exceptional performance and dominance in various fields, including natural language processing (NLP),^{15,16} medical imaging analysis,^{17,18} and chemical and biological research,^{19,20} garnering widespread recognition and acclaim for its capabilities.

Prompt engineering has become a crucial technique in LLMs for optimizing and fine-tuning them to perform specific tasks and achieve desired outcomes. This technique involves creating high-quality prompts that guide LLMs to generate accurate results.^{21,22} The process involves selecting the appropriate type of prompt, adjusting their size and structure, and sequencing them effectively according to the task requirements. Zheng *et al.* used prompt engineering to guide GPT-3.5 in extracting synthetic texts from the literature related to Metal–Organic Frameworks (MOFs) with a precision accuracy exceeding 90%.²³ Afterwards, the same group also used a prompt-learning

^aDepartment of Chemistry, Zhejiang University, Hangzhou, Zhejiang 310058, China. E-mail: mingliu@zju.edu.cn^bZJU-Hangzhou Global Scientific and Technological Innovation Center, Zhejiang University, Hangzhou, Zhejiang 311200, China^cKey Laboratory of Precision and Intelligent Chemistry, University of Science and Technology of China, Hefei, Anhui 230026, China. E-mail: linjiangchen@ustc.edu.cn^dSchool of Chemistry, School of Computer Science, University of Birmingham, Birmingham B15 2TT, UK† Electronic supplementary information (ESI) available. See DOI: <https://doi.org/10.1039/d4dd00337c>

‡ Equal contribution.



strategy to facilitate MOF material synthesis experiments through a symbiotic human-AI collaboration.²⁴ They later applied a similar approach to guide the discovery and optimization of synthesis conditions for MOFs and Covalent Organic Frameworks (COFs).²⁵ In 2024, Lu *et al.* successfully predicted the yield of ammonia catalytic reduction with up to 86% accuracy by incorporating pre-existing experimental data in the prompt project.²⁶

In this study, we employed prompt engineering to guide GPT-4 in performing multi-label text classification, a task more complex than binary classification and a significant challenge for large language models. Literature paragraphs were labeled based on the information they contained, such as authors, cage names, synthetic procedures, surface area, and the CCDC number of the corresponding cages. These labeled paragraphs were then used as the input for GPT-4 to extract and tabulate information into the cage knowledge database. Each row in the database contains details such as the cage name, corresponding synthetic procedures, monomers and their synthesis procedures, cage stoichiometry, surface area, and CCDC number. The accuracy of GPT-4's multi-label classification and information extraction was assessed by comparing its results with manually curated data, which served as the ground truth. Ultimately, the cage knowledge database was used to develop a chatbot capable of reliably answering a variety of cage-related questions.

Methodology

While the GPT model has shown promising performance for various linguistic tasks,^{15–20} directly using it to read entire bodies of literature and extract specific information about POCs presents significant challenges. To address this, we implemented a two-step process for literature analysis using GPT-4 (Fig. 1), consisting of multi-label text classification followed by information extraction.

In the first step, the articles were divided into text segments. Each text segment was assigned a categorical label using a GPT-

4 model trained with prompt engineering techniques (ESI, Section S2†). Since topology is described in a well-defined and fixed format, Python code was employed to identify specific sequences, as this method is more cost-effective compared to using GPT-4. In the second step, the selected text containing relevant information was further organized into tabulated data by both human experts and GPT-4. The verified answers were then compiled into a database, which was subsequently used for constructing chatbots.

Preparation of literature

We searched for literature in the Web of Science database using the keyword 'porous organic cage'. Literature that focuses only on applications of reported POCs rather than synthesis of new POCs was excluded, resulting in 153 articles. These papers were authored by 34 different research groups and published across seven publishers to ensure diversity in writing styles and formats. The POCs covered are primarily imine-type cages, with a smaller portion consisting of alkyne-type cages, aryl ether-type cages, and others.

GPT-based multi-label text classification

In this step, selected POC literature was segmented into paragraphs and labeled using a prompt-engineered GPT-4 model. We used PyPDF2 code to convert the pdf file into a split text, and then the symbols at the end of the text was used to determine whether the text is the end of a sentence.²⁷ If it is not the end, it is connected to the next text. This operation combines several text segments in a logical manner, thereby reducing the number of segments to be processed. A set of prompts was developed to train GPT-4 to generate labels for each paragraph, focusing on key aspects required by chemists, such as authors, affiliations, synthetic procedures, surface area, and CCDC numbers. To reduce ambiguity during labeling and filter out texts with insufficient information, additional categories were included, such as incomplete synthesis, additional authors, references, and others. The explanation for each label is provided in

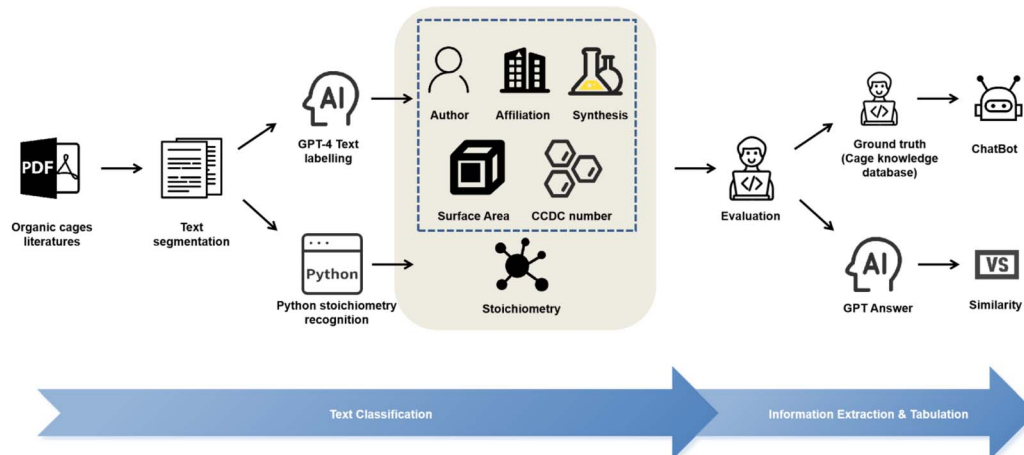


Fig. 1 The workflow of GPT-based information extraction from the literature. The workflow of GPT-based information extraction from the literature.



Table 1 Detailed description of each category

Category	Description	Required
Comprehensive synthesis	Contained comprehensive experimental conditions of the chemical reaction. The chemical reaction conditions must appear with clear information about the reaction temperature, reaction time, reactants, products, solvents, and their amounts	✓
CCDC	Contained CCDC number	✓
Surface area	Contained information on the specific surface area of a compound	✓
This paper's authors	Contained information about the authors of this paper	✓
Affiliation	Contained information about the authors' organizations, cities, nationalities <i>etc.</i>	✓
Extra authors	Contained authors of other articles, such as background descriptions	
Incomprehensive synthesis	Contained incomprehensive experimental conditions of the chemical reaction	
References	Contained references	
Others	Paragraphs that exceed all of the previously mentioned categories	

Table 1. For each labeling task, we devised 2–3 prompts per label, as detailed in ESI, Section S2.† We manually labelled each paragraph to serve as ground truth. The accuracy of the GPT-4 labelling was then assessed by comparing it to the ground truth, and evaluated using precision, recall, and F1 score.

Precision and recall were calculated as follows:

$$\text{Precision} = \frac{\text{TP}}{\text{TP} + \text{FP}}$$

$$\text{Recall} = \frac{\text{TP}}{\text{TP} + \text{FN}}$$

where TP, FP, and FN represent True Positive, False Positive, and False Negative, respectively.

The F1 score is a reconciled average of precision and recall:

$$\text{F1 score} = \frac{2}{\frac{1}{\text{Precision}} + \frac{1}{\text{Recall}}}$$

Information extraction & tabulation

All the paragraphs labeled with authors, affiliations, synthesis procedures, surface area, topology and CCDC numbers during the manual labelling process were used as textual input for GPT-4 to extract and tabulate relevant information, regardless of whether GPT-4 correctly classified the paragraphs. This process resulted in a POC database that improved the quality of the data, enabling more efficient interpretation and analysis. Each entry in the database systematically summarizes the relevant information, ensuring that key details—such as the cage name, topology, surface area, CCDC number, cage synthesis, monomer names, and monomer synthesis—are presented in a coherent and standardized format. We also manually extracted the same type of information as the cage knowledge database for the evaluation of GPT-4. The GPT-generated table was then compared with our manually created cage knowledge database using the Bidirectional Encoder Representation from Transformers (BERT) score. The BERT score is calculated as follows: the generated text and the reference text are encoded in the BERT model to obtain their respective vector representations. Subsequently, the similarity of two input texts is

calculated by computing the cosine similarity of the vector representation for each of the two words.²⁸

Database utilization and analysis

Having utilized text mining techniques to construct a cage knowledge database, our aim was to leverage this resource to its fullest potential. The cage knowledge database was then fed to a prompt-engineered GPT-4 assistant, enabling it to answer questions based on the database. Additionally, a user interface was built using Tkinter, a python's open source graphical User Interface (GUI) platform.²⁹ In order to fully explore the value of the database, we conducted statistical analysis of the synthesis strategy, topology, crystal structure from CCDC, and surface area in the database.

Results and discussion

Text classification

In the multi-label text classification, as shown in Fig. 2a, all text segments were processed by GPT-4 with prompt engineering. Labels were then generated and evaluated by comparing them with manually labeled text, which served as the standard, to assess the accuracy of the GPT-4 model.

Fig. 2b shows the distribution of different text categories, revealing that most of the text in the original documents falls under the categories of references and other sections. The key information we needed—such as authors, affiliations, specific surface areas, CCDC numbers, and experimental procedures—constitutes less than 10% of the total text content. This indicates that the GPT-4 classification process significantly reduces the volume of text to be processed in the tabulation step, lowering the corresponding costs.

The recall and precision results are illustrated in Fig. 2c. The “comprehensive synthesis” category had the highest recall rate at 0.74, which can be attributed to distinctive markers in the text, such as frequently mentioned compound names and amounts. However, there was a significant drop in precision for this category, down to 0.61. Observing the actual-*versus*-predicted category matrix (ESI, Fig. S1†), the primary error came from misidentifying segments that should have been labeled as “incomprehensive synthesis” as “comprehensive synthesis”.



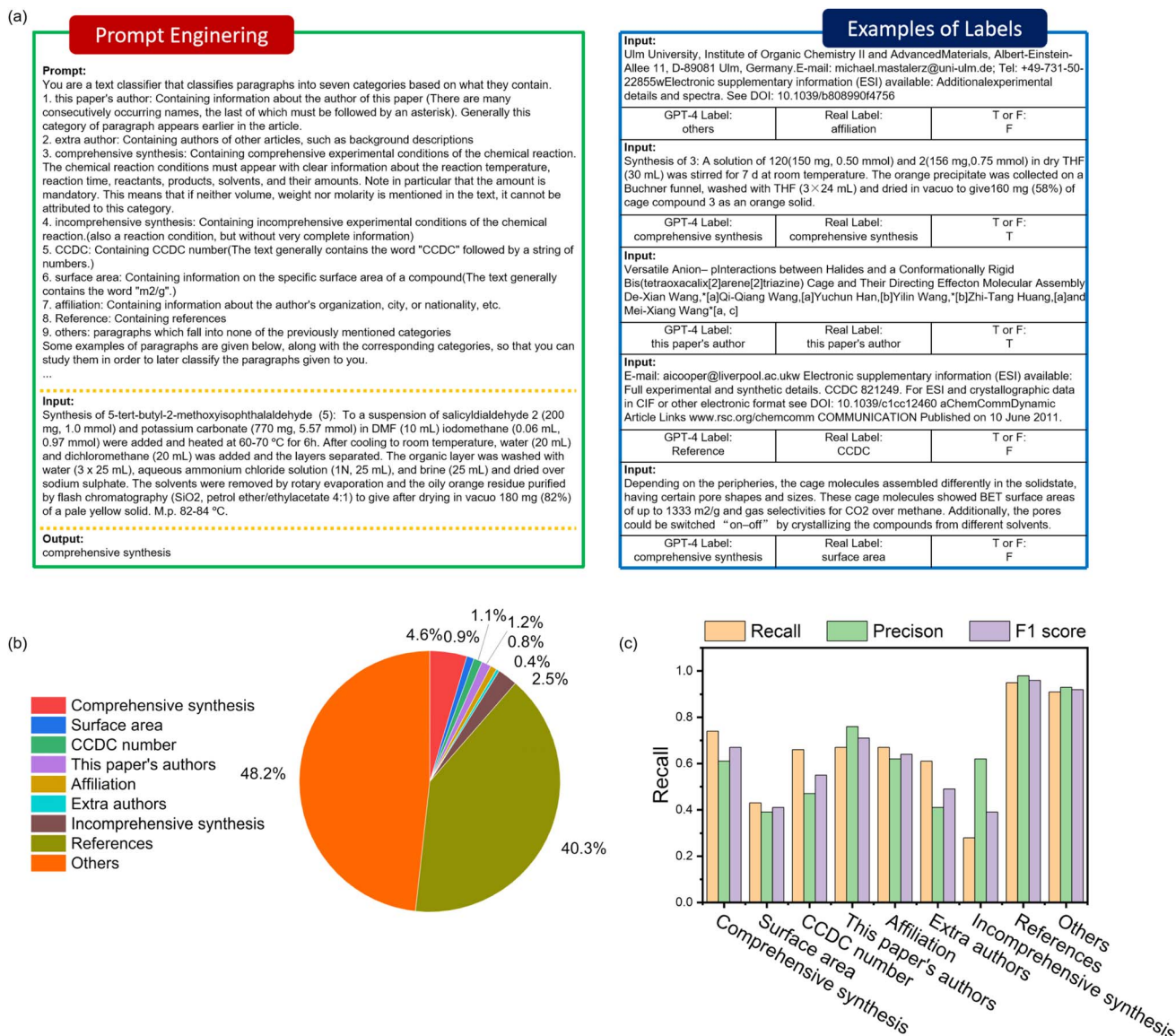


Fig. 2 Examples of prompt engineering and labels in text classification (a), visualization of the percentage distribution of various categories (b), and the recall values for each category and overall (c).

This highlights that even with prompt engineering designed to differentiate between comprehensive and incomprehensive synthesis, some errors persist. Texts under the “this paper’s authors”, “Affiliation”, and “CCDC number” categories had similar recall rates of 0.67, 0.67, and 0.66, respectively. However, the precision for “this paper’s authors” was notably higher than for “Affiliation” and “CCDC number”, showing a marked difference between precision and recall. Specific surface area information had both low recall and precision, likely because, while it has the identifier “m² g⁻¹”, it is often confused with similar terms like “m² s⁻¹” and “m/z”. The recall and precision of the surface area and CCDC numbers, which should be readily identifiable due to their distinct identifiers, were found to be unsatisfactory. This outcome can be attributed to redundant texts significantly interfering with the encoding and decoding process of GPT-4. Evidence for this conclusion is present in the

actual-versus-predicted category matrix (ESI, Fig S1†), which shows that the recall of CCDC is 66.44%, with 25.17% of the information misclassified as “others.” Similarly, the recall for surface area is 47.71%, while information classified as “others” accounts for 43.13%, a value comparable to the recall.

Information extraction & tabulation

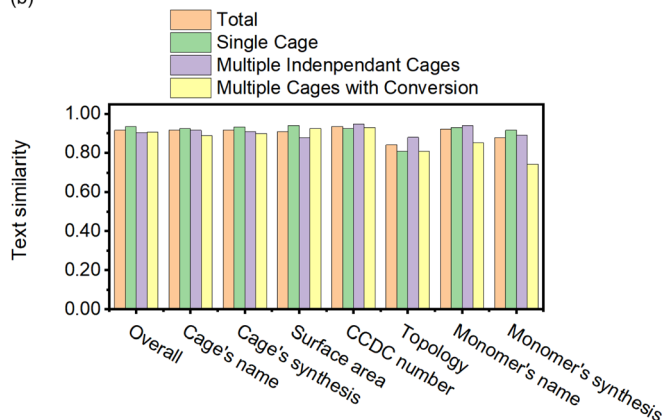
A typical example of tabulated information compiled from an article by both manual work and GPT-4 is shown in Fig. 3a for comparison. As observed, there is considerable similarity between the GPT-4 output and the manual results, with many matching parts and only minor differences. The name, topology and CCDC number of the molecular cages were accurately extracted with 100% text similarity. For the other sections, text similarity was less than 100%. These differences can be easily



(a)

	Manual Answer	GPT-4 Answer	BERT score
Cage Name	BPPOC	BPPOC	1.000
Topology	[3+6]	Herein, a new single-crystal [3 + 6] topological POC (BPPOC) was obtained from the condensation between 3 equiv 2,2'-bipyridine-based tetraaldehyde (BPDDP) molecules and 6 equiv R,R-cyclohexanediamine molecules, catalyzed by trifluoroacetic acid.	1.000
CCDC Number	2143974	2143974	1.000
Surface Area	BPPOC displays very low N ₂ uptake at even 1.0 bar, giving a low Brunauer-Emmett-Teller (BET) surface area of 52 m ² /g; Instead, on the basis of CO ₂ adsorption data at 196 K, the BET surface area of BPPOC is 577 m ² /g.	BPPOC displays very low N ₂ uptake at even 1.0 bar, giving a low Brunauer-Emmett-Teller (BET) surface area of 52 m ² /g. Instead, on the basis of CO ₂ adsorption data at 196 K, the BET surface area of BPPOC is 577 m ² /g, similar to that of BTPOC (605 m ² /g) under the same test conditions.	0.906
Cage Synthesis	To a suspension of BPDDP (210.2 mg, 0.5 mmol) and TFA (5.0 μL) in dichloromethane (450.0 mL), a solution of chiral R,R-cyclohexanediamine (125.6 mg, 1.1 mmol) in dichloromethane (50.0 mL) was added slowly and stirred at room temperature. After 48 h, the reaction mixture was filtered. The filtrate was then evaporated under reduced pressure. Recrystallization of the crude product in dichloromethane and methanol led to the precipitation of the target organic cage as a light yellow powder, which was dried at room temperature, giving BPPOC in the yield of 81% (209 mg).	Synthesis of BPPOC. To a suspension of BPDDP (210.2 mg, 0.5 mmol) and TFA (5.0 μL) in dichloromethane (450.0 mL), a solution of chiral R,R-cyclohexanediamine (125.6 mg, 1.1 mmol) in dichloromethane (50.0 mL) was added slowly and stirred at room temperature. After 48 h, the reaction mixture was filtered. The filtrate was then evaporated under reduced pressure. Recrystallization of the crude product in dichloromethane and methanol led to the precipitation of the target organic cage as a light yellow powder, which was dried at room temperature, giving BPPOC in the yield of 81% (209 mg).	0.958
Monomers	2,2'-bipyridine-based tetraaldehyde (BPDDP); R,R-cyclohexanediamine	5,5'-([2,2'-Bipyridine]-5,5'-diyl)-diisophthalaldehyde (BPDDP); R,R-Cyclohexanediamine	0.937
Synthesis of Monomers	A mixture of 5,5'-dibromo-2,2'-bipyridine (628.0 mg, 2.0 mmol), 5-(4,4,5,5-tetramethyl-1,3,2-dioxaborolan-2-yl)isophthalaldehyde (1100.0 mg, 4.2 mmol), potassium carbonate (1000.0 mg, 7.2 mmol), tetrakis(triphenylphosphine)palladium (150.0 mg, 0.1 mmol), tetrahydrofuran (18.0 mL), and water (2.0 mL) in a 50 mL flask was stirred at 95 °C under a nitrogen atmosphere. After 24 h, the reaction mixture was cooled to room temperature and filtered. The crude product was washed with eachwater (10.0 mL), tetrahydrofuran (10.0 mL), and methanol (10.0 mL) and finally dried at room temperature, according BPDDP (ca. 700mg) with a yield of 83%. None	Synthesis of 5,5'-([2,2'-Bipyridine]-5,5'-diyl)-diisophthalaldehyde. A mixture of 5,5'-dibromo-2,2'-bipyridine (628.0 mg, 2.0 mmol), 5-(4,4,5,5-tetramethyl-1,3,2-dioxaborolan-2-yl)isophthalaldehyde (1100.0 mg, 4.2 mmol), potassium carbonate (1000.0 mg, 7.2 mmol), tetrakis(triphenylphosphine)palladium (150.0 mg, 0.1 mmol), tetrahydrofuran (18.0 mL), and water (2.0 mL) in a 50 mL flask was stirred at 95 °C under a nitrogen atmosphere. After 24 h, the reaction mixture was cooled to room temperature and filtered. The crude product was washed with water (10.0 mL), tetrahydrofuran (10.0 mL), and methanol (10.0 mL) and finally dried at room temperature, affording BPDDP (ca. 700 mg) with a yield of 83%. None	0.939

(b)



(c)

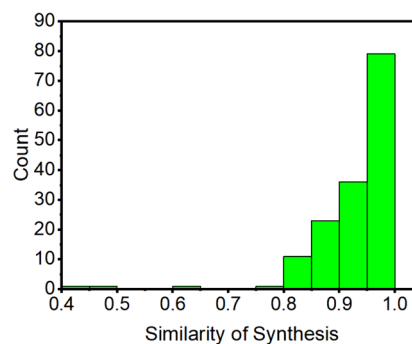


Fig. 3 A typical example of tabulated information generated by GPT-4 from one paper (a), the similarities between GPT-4 and manual information extraction (b), and the distribution of synthesis context similarity (c).

identified by comparing the two texts visually. To facilitate this comparison, Fig. 3a highlights the differing text portions in red.

For the monomers, differences arose in the naming of the same compound (BPDDP), while other differences were primarily due to redundant text being extracted by GPT-4. Specifically, GPT-4 included titles along with the synthetic routes for cages and monomers, while manual work did not. Regarding surface area, GPT-4's response included more information than the manual response, providing additional comparisons of surface area between BPPOC and another compound, BTPOC. This suggests that GPT-4 has the potential to offer additional information, enhancing researchers' understanding of cage-related knowledge.

The results of the BERT score calculation, shown in Fig. 3b, indicate that the average similarity score across all information in the articles was 0.9155. In particular, with a score of 0.9357, the CCDC numbers showed the highest similarity. The similarity scores for specific surface area, synthetic routes of molecular cages, names and synthetic routes of monomers were also relatively high, each reaching a value of around 0.90. The lowest similarity score of 0.8405 was observed for the information related to the topology, mainly because a significant part of the relevant information could not be successfully extracted from the text and was therefore labelled as "None".

Based on the complexity of their synthesis, the articles studied were systematically categorized into three different



classes: class I represents articles in which only a single POC has been reported; class II represents articles reporting multiple POCs without transformation relationships between them, usually synthesized in parallel using the same reaction type but different building blocks; class III represents articles that reported multiple POCs with transforming relationships among them. Analysis of the statistical graph shows a trend that, in general, the accuracy of information extraction gradually decreases as the complexity of the articles increases. However, in the extraction of topologies, articles in the second class had a considerably higher similarity than those in the first class, contrary to the general trend.

The distribution of similarity was further analyzed using the molecular cage synthetic route as a representative example (Fig. 3c). The analysis shows that most similarities are above 0.8, with a significant proportion exceeding 0.9. However, a few samples had notably lower similarity. Upon reviewing these cases, we found that low similarity scores were mainly due to unsuccessful extractions, resulting in a single word “None” or very short answers. A typical example of this error was the vague description “Condensation of a pyridine system” replacing a comprehensive synthesis route. Fortunately, such instances are rare and do not significantly impact GPT-4’s overall performance.

In the task of information extraction and tabulation, GPT-4 demonstrated strong capabilities in processing input text and extracting multiple categories of information simultaneously. This feature can significantly aid researchers by allowing for quicker reading and summarization of new papers. With GPT-4’s assistance, researchers can save considerable time and effort

in literature review, enabling them to focus more on tasks that require innovation and creativity.

Database utilization of the chatbot

Fig. 4a demonstrates that the GPT-4 model can effectively study and interpret the database to respond to user queries, as shown in a classic example. When asked about the reducing agent for the conversion of CC3 to RCC3, GPT-4 provided the correct answer “NaBH₄” based on our knowledge. Additionally, GPT-4 not only provided synthetic routes with detailed information about reactants, solvents, and catalysts but also included methodologies for synthesizing reactants when detailed experimental procedures are requested. Beyond simple questions related to a single research paper, the chatbot can also address more complex queries. However, when faced with more systematic and intricate questions, the accuracy and completeness of the answers tend to decline. Fig. 4b highlights this issue: when prompted to list all the molecular cages documented by a specific scientist, the chatbot produced only 16 responses, failing to generate the complete list of 59 entries. Repeated experiments have confirmed that this outcome is not due to randomness but stems from the limitations of GPT-4. Although GPT-4 has a context limit of up to 128K, it still struggles to effectively process lengthy dialogues or texts.³⁰

These results offer substantial evidence that GPT-4 is capable of answering questions based on the information contained within the database. The types of questions it can address are diverse and not limited to a specific subset. GPT-4’s responses are comprehensive enough to aid chemists in obtaining relevant information without the need to read the full text. Additionally,

(a) User: What is the **reducing agent** for the conversion of CC3 to RCC3?
 Assistant: The reducing agent used for the conversion of CC3 to RCC3 is **sodium borohydride (NaBH₄)**.
 User: Please tell me briefly the **exact synthesis route**.
 Assistant: 1. Dissolve the imine cage **CC3-R** (926 mg, 0.83 mmol) in a chloroform/methanol mixture (1:1 v/v, 50 mL) and stir until the solution becomes clear.
 2. Add **sodium borohydride** (1.00 g, 26.5 mmol) to the clear solution and stir for 12 hours at room temperature.
 3. Add water (2 mL) to the reaction mixture and stir for an additional 12 hours.
 4. Remove the solvent under vacuum.
 5. Extract the resulting white solid with chloroform (2 × 50 mL).
 6. Combine the organic phase and wash it with water (2 × 100 mL).
 7. Dry the chloroform phase using anhydrous magnesium sulfate (MgSO₄) before removing it under vacuum.
 8. RCC3 (crude yield = 900 mg, 95.1%) is obtained as a white solid.
 9. Purify RCC3 using a reversible reaction with acetone:
 - Dissolve 1000 mg of crude **RCC3** in 100 mL of acetone and allow the solution to stand.
 - Crystals start to appear on the wall of the flask after 30 minutes.
 - Collect the crystals (AT-RCC3) after one day by filtration.
 - Dissolve the crystals again in a chloroform/methanol mixture (1:1 v/v) and stir.
 - Add several drops of distilled water to the solution and stir for another 12 hours.
 - Remove the solvents to recover pure **RCC3** (680 mg, 70.4%).
 This process effectively converts CC3 to RCC3 using sodium borohydride as the reducing agent.

(b) User: Please list all molecular cages reported by **Prof. Andy Cooper** (name and article title only)
 Assistant: Here are the molecular cages reported by Prof. Andy Cooper along with the respective article titles:
 1. **Cage Name: CC7**
 - **Article Title:** Large Self-Assembled Chiral Organic Cages: Synthesis, Structure, and Shape Persistence
 2. **Cage Name: CC8**
 - **Article Title:** Large Self-Assembled Chiral Organic Cages: Synthesis, Structure, and Shape Persistence
 3. **Cage Name: TC1 [3+3]**
 - **Article Title:** Cage Doubling: Solvent-Mediated Re-equilibration of a [3 + 6] Prismatic Organic Cage to a Large [6 + 12] Truncated Tetrahedron
 4. **Cage Name: CC20**
 - **Article Title:** Synthesis of a Large, Shape-Flexible, Solvatomorphic Porous Organic Cage
 5. **Cage Name: CC13**
 - **Article Title:** Controlling the Crystallization of Porous Organic Cages: Molecular Analogs of Isorectical Frameworks Using Shape-Specific Directing Solvents
 6. **Cage Name: CC10**
 - **Article Title:** Supramolecular engineering of intrinsic and extrinsic porosity in covalent organic cages
 7. **Cage Name: CC9**
 - **Article Title:** Supramolecular engineering of intrinsic and extrinsic porosity in covalent organic cages
 8. **Cage Name: Cage 3-R**
 - **Article Title:** Modular and Predictable Assembly of Porous Organic Molecular Crystals
 9. **Cage Name: CC12**
 - **Article Title:** Shape Prediction for Supramolecular Organic Nanostructures: [4 + 4] Macrocylic Tetrapods
 10. **Cage Name: Cage 5-R**
 - **Article Title:** Supramolecular engineering of intrinsic and extrinsic porosity in covalent organic cages
 11. **Cage Name: CC11**
 - **Article Title:** Shape Prediction for Supramolecular Organic Nanostructures: [4 + 4] Macrocylic Tetrapods
 12. **Cage Name: CC6**
 - **Article Title:** Selective Gas Sorption in a [2+3] "Propeller" Cage Crystal
 13. **Cage Name: CC18**
 - **Article Title:** Periphery-Functionalized Porous Organic Cages
 14. **Cage Name: Cage 3**
 - **Article Title:** Porous Organic Cages
 15. **Cage Name: TC1-R**
 - **Article Title:** Reticular Synthesis of Porous Molecular 1-Dimensional Nanotubes and 3-Dimensional Networks
 16. **Cage Name: TC3-R**
 - **Article Title:** Reticular Synthesis of Porous Molecular 1-Dimensional Nanotubes and 3-Dimensional Networks

Fig. 4 Illustration of the interactive dialogue system underpinned by the GPT-4 model which demonstrates the high capacity to generate and refine responses for simple questions (a) and limited capacity to generate partially correct response for more systematic and intricate questions (b).



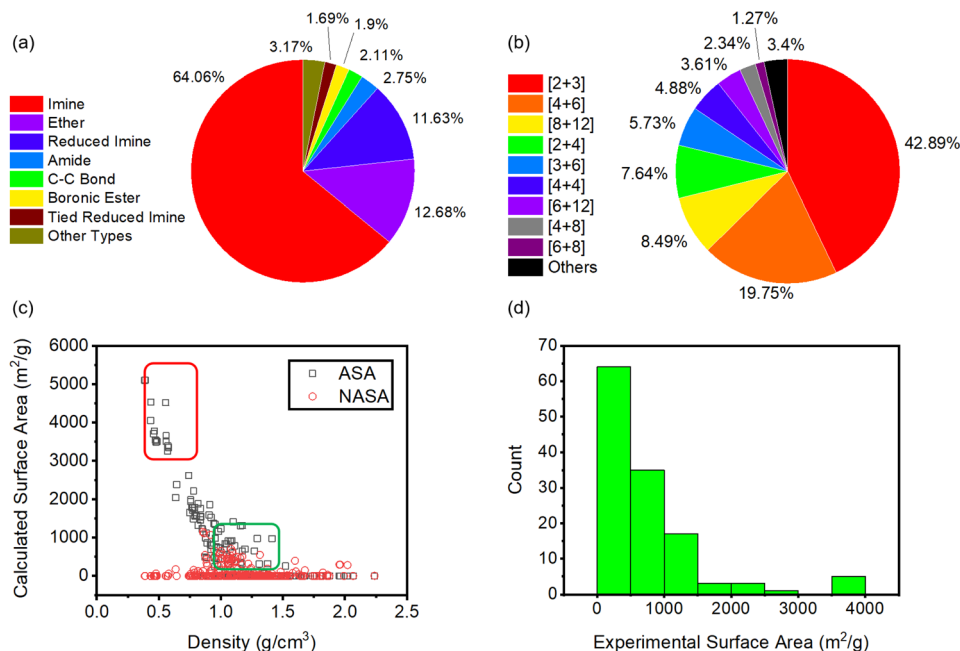


Fig. 5 Statistical analysis of the chemistries involved in synthesis (a), topology (b), CCDC structures (c) and surface areas (d) of cages.

the system can meet practical demands in the field, such as providing detailed guidance for the synthesis of organic cages.

Database analysis

In order to summarize the information in the database, the synthetic chemistries, topologies, crystallographic structures, and surface areas of the entries were analyzed.

Approximately 64% of the cages in the database were formed *via* imine condensation, with 11.63% being reduced from these imine precursors. This indicates that imine chemistry currently dominates the synthesis of porous organic cages (POCs). Additionally, 12.68% of the cages were synthesized *via* ether bonds, while other synthetic methods, such as amides and boronic esters, were also observed (Fig. 5a).

In terms of topologies, the analysis shows that [2 + 3]-cages account for 42.89%, which is nearly half of all entries in the database. Additionally, [4 + 6]-cages and [8 + 12]-cages are relatively prevalent, comprising 19.75% and 8.49% of the total, respectively (Fig. 5b).

Surface area provides guidance for exploring cage porosity and identifying potential applications. The density and accessible surface area (ASAs) of 253 entries were calculated using the Zeo++ software package (Fig. 5c).³¹ The probe radius was set as 1.82 Å, which is the kinetic radius of a nitrogen molecule. The results revealed a negative correlation between density and accessible surface area (ASA). Lower densities, around 0.5 g cm⁻³, correspond to ASAs exceeding 3000 m² g⁻¹ (red circle, Table S2†). Non-accessible surface area (NASA) values are generally lower, with significant values observed only within the density range of 1.00–1.25 g cm⁻³ (green circle). This is due to the inherent low surface area of high-density crystal structures.

Analysis of experimental surface area data revealed that approximately 60 POCs exhibit surface areas exceeding 500 m² g⁻¹, with 12 entries surpassing 1500 m² g⁻¹ (Fig. 5d). With the exception of a boronic ester-based cage, all high-surface-area cages were imine-based. This suggested that imine-based cages are currently one of the most promising methods for achieving high surface areas.

Conclusions

In this study, we developed a GPT-based system for extracting information from academic literature focused on organic molecular cages, resulting in a comprehensive molecular cage information database. Specifically, we evaluated the proficiency of the GPT-4 model in extracting and organizing detailed data on organic molecular cages from a large body of scientific literature. The resulting database, along with the associated interactive dialogue system, offers a valuable resource for advancing research in the design, synthesis, and application of molecular cages. Furthermore, the database created in this work provides a crucial resource for future machine learning and experimental studies aimed at discovering new POCs. However, the dialogue system shows limitations in answering more complex questions. Future efforts will focus on enhancing the search capabilities of the system. Additionally, the database can be updated dynamically, allowing newly reported organic molecular cages to be incorporated through the process outlined in this article. Looking forward, LLMs, in conjunction with other rapidly evolving AI tools and lab-automation techniques, have the potential to significantly accelerate the discovery of new molecules, such as POCs and beyond.



Data availability

The data supporting this article can be found in the ESI. Raw data, the resulting database of POCs and custom codes for this work, including scripts for the directly runnable chatbot, as well as the results of text classification and information tabularization, are available at <https://doi.org/10.5281/zenodo.14511583>. The version of the code employed for this study is Version v1. The codes are also available at <https://github.com/syy1213/LLMs-GPT-4-Cage>.

The codes and required python modules for text classification, information tabularization and the directly runnable chatbot can be found at https://hub.docker.com/r/syy12137059/cage_gpt/tags.

Author contributions

Yaoyi Su: investigation, formal analysis, validation and writing – original draft. Siyuan Yang: conceptualization, methodology, supervision and writing – review & editing. Yuanhan Liu and Aiting Kai: resources and validation. Linjiang Chen and Ming Liu: project administration, supervision, funding acquisition and writing – review & editing.

Conflicts of interest

There are no conflicts to declare.

Acknowledgements

The authors thank the National Natural Science Foundation of China (22371252) and the Zhejiang Provincial Natural Science Fund (LZ23B020005), and are thankful for the Leading Innovation Team grant from the Department of Science and Technology of Zhejiang Province (2022R01005).

Notes and references

- 1 T. Tozawa, J. T. A. Jones, S. I. Swamy, S. Jiang, D. J. Adams, S. Shakespeare, R. Clowes, D. Bradshaw, T. Hasell, S. Y. Chong, C. Tang, S. Thompson, J. Parker, A. Trewin, J. Bacsa, A. M. Z. Slawin, A. Steiner and A. I. Cooper, *Nat. Mater.*, 2009, **8**, 973–978.
- 2 S. Jiang, J. Bacsa, X. F. Wu, J. T. A. Jones, R. Dawson, A. Trewin, D. J. Adams and A. I. Cooper, *Chem. Commun.*, 2011, **47**, 8919–8921.
- 3 J. M. Lucero and M. A. Carreon, *ACS Appl. Mater. Interfaces*, 2020, **12**, 32182–32188.
- 4 K. Z. Su, W. J. Wang, S. F. Du, C. Q. Ji and D. Q. Yuan, *Nat. Commun.*, 2021, **12**, 3703.
- 5 Y. X. Chen, G. C. Wu, B. B. Chen, H. Qu, T. Y. Jiao, Y. T. Li, C. Q. Ge, C. Zhang, L. X. Liang, X. Q. Zeng, X. Y. Cao, Q. Wang and H. Li, *Angew. Chem., Int. Ed.*, 2021, **60**, 18815–18820.
- 6 C. Zhang, H. Y. Wang, J. Zhong, Y. Lei, R. F. Du, Y. Zhang, L. B. Shen, T. Y. Jiao, Y. L. Zhu, H. M. Zhu, H. R. Li and H. Li, *Sci. Adv.*, 2019, **5**, eaax6707.
- 7 P. Bhandari and P. S. Mukherjee, *ACS Catal.*, 2023, **13**, 6126–6143.
- 8 L. Qiu, R. McCaffrey, Y. H. Jin, Y. Gong, Y. M. Hu, H. L. Sun, W. Park and W. Zhang, *Chem. Sci.*, 2018, **9**, 676–680.
- 9 S. Jiang, H. J. Cox, E. I. Papaioannou, C. Y. Tang, H. Y. Liu, B. J. Murdoch, E. K. Gibson, I. S. Metcalfe, J. S. O. Evans and S. K. Beaumont, *Nanoscale*, 2019, **11**, 14929–14936.
- 10 B. Dietrich, J. M. Lehn and J. P. Sauvage, *Tetrahedron Lett.*, 1969, **10**, 2885–2888.
- 11 T. Hasell and A. I. Cooper, *Nat. Rev. Mater.*, 2016, **1**, 16053.
- 12 D. Y. Hu, J. J. Zhang and M. Liu, *Chem. Commun.*, 2022, **58**, 11333–11346.
- 13 X. C. Yang, Z. Ullah, J. F. Stoddart and C. T. Yavuz, *Chem. Rev.*, 2023, **123**, 4602–4634.
- 14 OpenAI, <https://openai.com/>, accessed December 2024.
- 15 C. C. Chiang, M. Luo, G. Dumkrieger, S. Trivedi, Y. C. Chen, C. J. Chao, T. J. Schwedt, A. Sarker and I. Banerjee, *Headache*, 2024, **64**, 400–409.
- 16 S. Nath, A. Marie, S. Ellershaw, E. Korot and P. A. Keane, *Br. J. Ophthalmol.*, 2022, **106**, 889–892.
- 17 S. Ziegelmeier, A. W. Marka, N. Lenhart, N. Nehls, S. Reischl, F. Harder, A. Sauter, M. Makowski, M. Graf and J. Gawlitza, *J. Med. Internet Res.*, 2023, **25**, e50865.
- 18 I. Civettini, A. Zappaterra, B. M. Granelli, G. Rindone, A. Aroldi, S. Bonfanti, F. Colombo, M. Fedele, G. Grillo, M. Parma, P. Perfetti, E. Terruzzi, C. Gambacorti-Passerini, D. Ramazzotti and F. Cavalca, *Br. J. Haematol.*, 2024, **204**, 1523–1528.
- 19 G. V. Ye and J. Comput, *Aid, Mol. Des.*, 2024, **38**, 20.
- 20 Z. L. Zheng, Z. G. He, O. Khattab, N. Rampal, M. A. Zaharia, C. Borgs, J. T. Chayes and O. M. Yaghi, *Digital Discovery*, 2024, **3**, 491–501.
- 21 P. Korzynski, G. Mazurek, P. Krzypkowska and A. Kurasinski, *Entrep. Bus. Econ. Rev.*, 2023, **11**, 25–37.
- 22 S. Ayad and F. AlSayoud, *Lect. Note. Netw. Syst.*, 2024, vol. 987, pp. 412–422.
- 23 Z. L. Zheng, O. F. Zhang, C. Borgs, J. T. Chayes and O. M. Yaghi, *J. Am. Chem. Soc.*, 2023, **145**, 18048–18062.
- 24 Z. L. Zheng, Z. C. Rong, N. Rampal, C. Borgs, J. T. Chayes and O. M. Yaghi, *Angew. Chem., Int. Ed.*, 2023, **62**, e202311983.
- 25 Z. L. Zheng, O. F. Zhang, H. Nguyen, N. Rampal, A. H. Alawadhi, Z. C. Rong, T. Head-Gordon, C. Borgs, J. T. Chayes and O. M. Yaghi, *ACS Cent. Sci.*, 2023, **9**, 2161–2170.
- 26 M. Y. Lu, F. Y. Gao, X. L. Tang and L. J. Chen, *Iscience*, 2024, **27**, 109451.
- 27 *PyPDF2*, <https://pypi.org/project/PyPDF2/>, accessed December 2024.
- 28 J. Y. Lee, K. Jung and Pr. Mach, *Learn. Res.*, 2019, **101**, 1081–1093.
- 29 *Tkinter*, <https://docs.python.org/3/library/tkinter.html>, accessed December 2024.
- 30 *OpenAI*, <https://gpt40mni.com/safety-and-limitations/>, accessed December 2024.
- 31 T. F. Willems, C. H. Rycroft, M. Kazi, J. C. Meza and M. Haranczyk, *Microporous Mesoporous Mater.*, 2012, **149**, 134–141.

